Physisorption on TiO_2

1:1 and 2:1 Charge-Transfer Complexes between Aromatic Hydrocarbons and Dry Titanium Dioxide**

*You Seok Seo, Changhoon Lee, Kee Hag Lee, and Kyung Byung Yoon**

The unique properties of TiO_2 have made it a popular material for various extensive applications in, for example, solar cells,[1] water splitting,[2] water treatment,[3] photocatalysts,[4,5] superhydrophilic coatings,[5] sensors,[6] and batteries.[7] Since the first step in these applications involves the interaction between the TiO_2 surface and the adsorbate, understanding the nature of the interactions at the interface is essential for understanding the known properties and for exploring new applications.

Two types of interactions have been observed so far: coordinative covalent bonding (CCB)[8–15] between the adsorbates and the Ti^{IV} ions on TiO_2 surfaces and the physical adsorption (PA). The CCB-type interactions give rise to ligand-to-metal charge-transfer (LMCT) interactions between the adsorbates and Ti^{IV} ions, owing to the low-lying empty t_{2g} orbitals of the Ti^{IV} centers in octahedral environments. Indeed, those relatively electron-rich adsorbates having functional groups such as enediol (notably catechol,[8] ascorbic acid,[9] dopamine,[10] and alizarin[8c]), carboxylate (notably 4-(methylsulfanyl)benzoic acid[11] and sulfanylacetic acid[12]), nitrile (notably ferricyanide[13]), and alcohol (notably 4-hydroxybiphenyl[14]) groups display LMCT bands in the visible region. The less electron-rich adsorbates such as thiocyanate showed the corresponding LMCT band in the UV region.[15]

In contrast to the well-studied CCB-type interaction, however, nothing is known about the nature of interaction between the physically adsorbed molecules and TiO_2. Stemming from our interests on the charge-transfer (CT) interactions between the zeolite framework and intercalated guest molecules,[16] we have conducted a series of experiments to study the interaction between TiO_2 and the adsorbates. As a result, we have discovered that pure polycyclic hydrocarbon arenes (ArHs) readily form 1:1 and 2:1 CT complexes with dry TiO_2 surfaces.

When dry TiO_2 (anatase, average diameter = 50 nm) particles were suspended in dilute CH_2Cl_2 solutions of phenanthrene (**1**), chrysene (**2**), anthracene (**3**), pyrene (**4**), and benzo[*a*]pyrene (**5**, Figure 1) in a dry box, the TiO_2 particles immediately picked up pale brownish colors. The added amounts of ArHs correspond to 2–20% surface coverage of TiO_2 based on the monomeric forms. Upon removal of the solvent by evacuation in the dry box, the colors intensified significantly. The colored TiO_2 particles bleached back to colorless when they were washed with CH_2Cl_2, and the UV/Vis spectra of the rinses were identical to those of the pure ArHs (see the Supporting Information), indicating that the color generation is a reversible process, and the coloration is not the result of the degradation of the ArHs upon contact with TiO_2. On the contrary, coloration did not occur with dried SiO_2 and $BaSO_4$, emphasizing that the coloration is unique to TiO_2. The diffuse reflectance spectra of the colored, dry TiO_2 particles revealed the presence of new absorption bands whose onsets progressively red-shifted with decreases in the calculated vertical ionization potential (IP_V) of ArH (Table 1, Figure 2a).

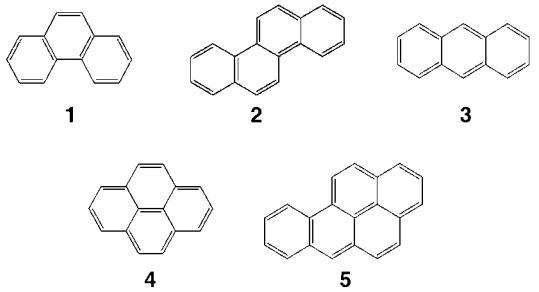

Figure 1. Structures of the aromatic hydrocarbons used in this study.

Deconvolution of the spectra (see the Supporting Information) revealed a new absorption in the case of phenanthrene (**1**) and two new absorption bands in the cases of more electron-rich arenes (Figure 2b). The two new absorption bands are designated as high-energy bands (HEBs) and low-energy bands (LEBs), respectively, and their energies at the absorption maximums ($E(\lambda_{max})$) are listed in Table 1. The new absorption band from **1** is classified as LEB based on the trend of other ArHs and by assuming that its HEB has shifted to the shorter wavelength UV region. The HEBs are unequivocally assigned as CT bands between ArH and TiO_2 based on the Mulliken linear relationship[17] between the calculated IP_V(ArH) and $E(\lambda_{max})$ as shown in Figure 3a.

LEBs were assigned as the CT bands between the arene dimers[18] and TiO_2, based on the following reasoning and evidence. First, it is well established that polycyclic ArHs readily form dimers $(ArH)_2$s on the hydrophilic solid surfaces when the surface coverage exceeds 1%.[19] Indeed, the diffuse reflectance spectra of the adsorbed ArHs on $BaSO_4$ were broader when the surface coverage was higher than 3%, and the onsets significantly red-shifted with respect to the

[*] Y. S. Seo, Prof. Dr. K. B. Yoon
Center for Microcrystal Assembly and
Department of Chemistry
Sogang University
Seoul 121-742 (Korea)
Fax: (+82) 2-706-4269
E-mail: yoonkb@sogang.ac.kr
C. Lee, Prof. Dr. K. H. Lee
Department of Chemistry and
Research Institute of Basic Science
Wonkwang University
Iksan, Jeonbuk 570-749 (Korea)

[**] We thank the Ministry of Science and Technology, Korea (Creative Research Initiatives Program) and Wonkwang University (2003) for supporting this work.

Supporting information for this article is available on the WWW under http://www.angewandte.org or from the author.

  DOI: 10.1002/ange.200461972

Table 1: IP_V and IP_A values of monomeric and dimeric arenes and energies of new absorption bands [eV].[a]

ArH	IP_V(ArH)	IP_A(ArH)		$IP_V[(ArH)_2]$	$IP_A[(ArH)_2]$	$E(\lambda_{max})$[a]	
	Calcd[b]	Calcd[b]	Expt[c]	Calcd[b]	Calcd[b]	HEB	LEB
1	8.08	7.89	7.89[d]	7.96	7.58		3.35
2	7.81	7.62	7.60[e]	7.50	7.21	3.41	2.99
3	7.65	7.51	7.44[d]	7.29(7.1)[f]	6.99(6.89)[f]	3.24	2.83
4	7.63	7.48	7.43[d]	7.27	6.99	3.23	2.84
5	7.33	7.16	7.12[d]	6.92	6.49	2.97	2.41

[a] Energy of new absorption bands at the absorption maximum. [b] Calculated values. [c] Experimentally determined values. [d] From ref. [21]. [e] From ref. [22]. [f] From ref. [23].

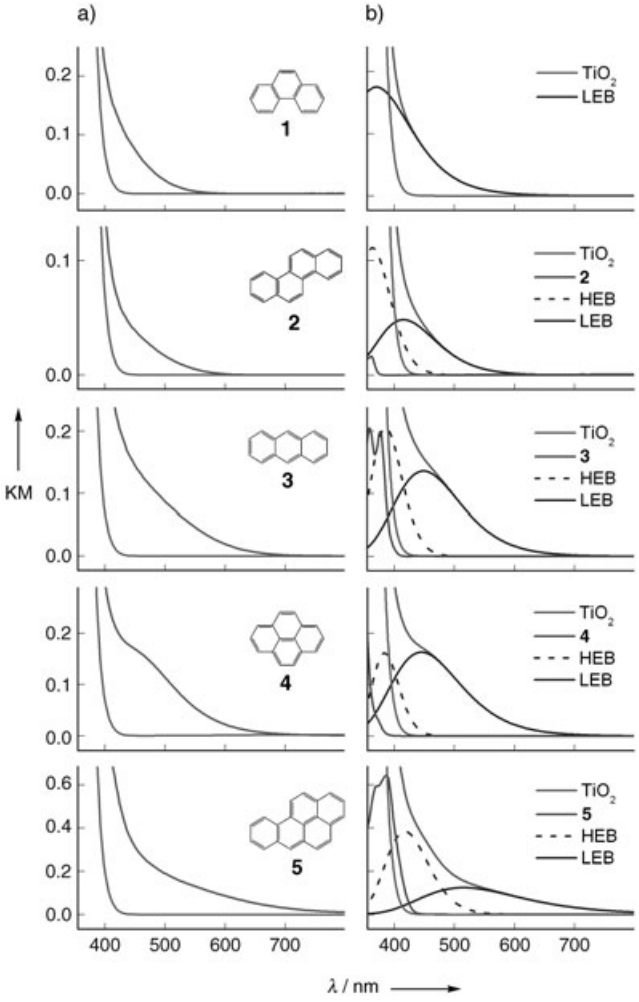

Figure 2. a) Diffuse reflectance UV/Vis spectra of TiO_2 (green curve) and arene-adsorbed TiO_2 (red curve) for each arene as indicated and b) the corresponding deconvoluted spectra. KM in the ordinate stands for the Kubelka–Munk value.

corresponding spectra in CH_2Cl_2 (see the Supporting Information), which is a characteristic feature of arene dimers. Furthermore, in the case of anthracene (**3**), the fluorescence spectrum on $BaSO_4$ displayed an excimer emission band at 420 nm (see the Supporting Information), which is another characteristic feature of the presence of $\mathbf{3}_2$.

By the same analogy, it is most likely that both ArH and $(ArH)_2$ coexist on the hydrophilic TiO_2 surface, although the obscuring CT bands make it difficult to identify the local bands of the two species. Second, the relative intensities of the LEBs increased when the surface coverage on TiO_2 was increased from 2% to 20% (see the Supporting Information). Last, most convincingly, there also exists an excellent Mulliken linear relationship between the calculated IP_V values of arene dimers (denoted as $IP_V[(ArH)_2]$) and the $E(\lambda_{max})$ values of LEBs (Table 1) as shown in Figure 3b.

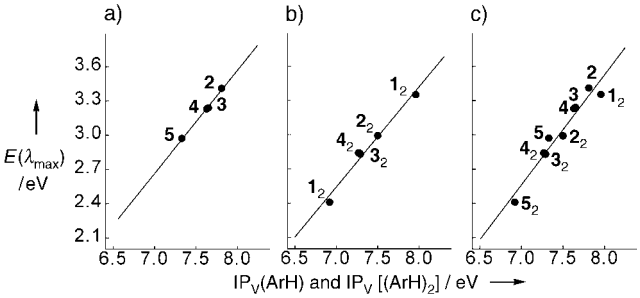

Figure 3. The Mulliken relationships between a) HEB and IP_V(ArH), b) LEB and $IP_V[(ArH)_2]$, and c) the combined values.

The formation of two CT bands also often occurs due to the transitions from the HOMOs (highest occupied molecular orbitals) and the HOMO-1s (second HOMOs) of the electron donors, respectively, to the LUMOs (lowest unoccupied molecular orbitals) of the electron acceptors. In this respect, as a possible means to check whether the two bands arise from the CT transitions from the HOMOs and HOMO-1s of ArHs, respectively, to the TiO_2 conduction band, we also obtained HOMO and HOMO-1 energy levels of the ArHs (see the Supporting Information). While the plot between HOMO energy levels and LEBs gave a linear relationship, the plot between HOMO-1 energy levels and HEBs showed no correlation whatsoever (see the Supporting Information), unambiguously showing that the HEBs do not arise due to the transition from HOMO-1 energy levels of ArH to the conduction band of TiO_2.

We therefore conclude that the arene donors form two types of CT complexes with dry TiO_2 surface, [ArH–TiO_2] and [$(ArH)_2$–TiO_2], as illustrated in Figure 4. The combined linear relationship (Figure 3c) was formulated as Equation (1),

$$E(\lambda_{max}) = 0.96\ IP_V(\text{arene}) - 4.18 \quad (1)$$

where IP_V(arene) represents both IP_V(ArH) and $IP_V[(ArH)_2]$. Interestingly, the observed correlation constant is close to 1 even though the CT interaction is heterogeneous in nature. From the energy level diagram shown in Figure 5, the average acceptor energy level of TiO_2 was deduced to be −4.45 eV, which is lower than the TiO_2 conduction band edge

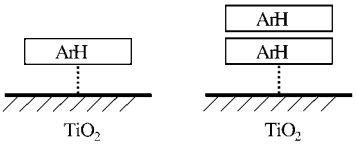

Figure 4. The two types of CT complexes formed by ArH on TiO_2.

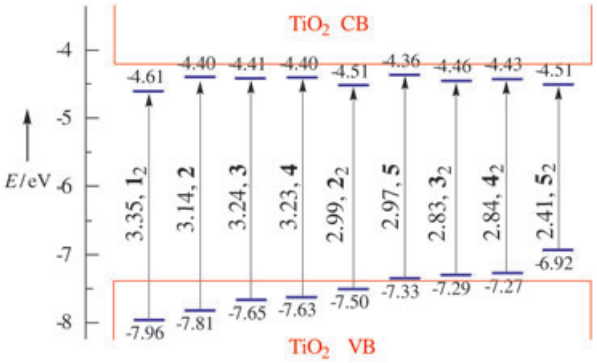

Figure 5. Energy level diagram of $IP_V(ArH)$, $IP_V[(ArH)_2]$, the conduction and valence bands of TiO_2, and the CT excitation energy.

(−4.2 eV)[20] by 0.25 eV. This indicates that the acceptor sites are mostly the defect or trap sites of the TiO_2 particles.

We also listed the calculated adiabatic ionization potentials (IP_A) of the arene monomers and dimers in Table 1. The $IP_A(ArH)$ values are very close to those determined experimentally,[21–23] thus demonstrating the reliability of our calculated IP_V and IP_A values. Although the $IP_A(ArH)$ and $IP_A[(ArH)_2]$ values also gave an excellent Mulliken plot with the $E(\lambda_{max})$ values of the LEBs and HEBs (see the Supporting Information), we used IP_V values in Figures 3 and 5, in compliance with the Mulliken CT theory.[17]

Unlike on $BaSO_4$ and SiO_2, the arenes did not fluoresce on TiO_2, most likely due to electron-transfer quenching, in support of the CT nature of the interaction. The CT bands quickly disappeared upon exposure of the colored, dry TiO_2 to moisture, indicating that moisture quickly intervenes between the hydrophilic TiO_2 surface and hydrophobic ArH or $(ArH)_2$, leading to breakage of arene–TiO_2 CT interaction (see the Supporting Information). The CT bands are also thermally and photochemically unstable most likely due to electron transfer from the arene monomers and dimers to TiO_2 (see the Supporting Information). The elucidation of the electron-transfer dynamics and the identification of the photoproducts are subjects of further study. This report thus reveals that the PA-type interaction between arenes and TiO_2 is a CT interaction in nature, suggesting that this type of interaction is general for other physically adsorbed molecules on TiO_2. The CCB- and PA-type interactions can be rephrased as inner- and outer-sphere CT interactions, respectively, according to the formulation of Kochi et al.[24] Thus, our finding leads to the conclusion that molecules form either inner- or outer-sphere CT complexes with TiO_2. Our finding also opens the possibility of using dry TiO_2 films in sensors and other useful devices.

Experimental Section

Titanium(IV) isopropoxide [Ti(O*i*Pr)$_4$] was purchased from Across and used as received. Tetramethylammonium hydroxide (TMAOH, 25% aqueous solution), compounds **1**–**5** were purchased from Aldrich and used as received. $BaSO_4$ was purchased from Matheson, Coleman, and Bell.

Preparation of TiO_2 (anatase) nanoparticles. TMAOH (25% solution, 6.92 g, 19 mmol) was dissolved in distilled deionized water (450 g, 25 mol) contained in a 1 L beaker. Ti(O*i*Pr)$_4$ (170.4 g, 25 mol) was dissolved in isopropyl alcohol (180 mL), and the Ti(O*i*Pr)$_4$ solution was slowly added dropwise to the TMAOH solution while it was rigorously stirred with the aid of a magnetic stirring bar. The milky, opaque gel was heated at 100 °C for 3 h with vigorous stirring until the solution became semitransparent. After addition of 200 mL of distilled deionized water to the gel, the gel was heated (at 100 °C) and stirred further until the total volume decreased to 450 mL, and the solution became transparent. The transparent gel was then transferred to a Teflon-lined autoclave, and the gel was heated at 180 °C for 5 h. After the gel was cooled to room temperature by immersing the autoclave in cold water, the gel was passed through a Whatman filter (pore size = 2.5 μm) to remove Teflon particles and other large particles. The gel was then dried under vacuum at room temperature and the remaining white mixture of TiO_2 nanoparticles and TMAOH was ground into a fine powder with a mortar and pestle. The finely ground mixture was calcined at 450 °C for 24 h to remove TMAOH and other organic residues. The identity of the calcined powder as anatase was confirmed by its X-ray diffraction pattern measured with a Rigaku D/MAX-1C instrument (see the Supporting Information). The surface area of the anatase particles was with a Micromeritics ASAP 2000 as 48 $m^2 g^{-1}$. The scanning electron microscope (SEM) image of the calcined TiO_2 particles showed the grains were ≈50 nm in diameter and that they exist as agglomerates (see the Supporting Information).

Formation of arene–TiO_2 CT complexes. The calcined anatase particles (50 g) were introduced into a cylindrical glass flask equipped with a vacuum adaptor, and the particles were evacuated at 200 °C for 12 h at $< 10^{-5}$ torr. The airtight glass container was then transferred into a dry box charged with high-purity argon and stored as such in the dry box. Typically, an aliquot of the anatase particles (1.3 g) was transferred into a 10-mL vial, and CH_2Cl_2 (2 mL) was introduced into the vial. The roomlight around the dry box was turned off, and most of the windowpane of the dry box was covered with black cloth. A weak red lightbulb was turned on around the uncovered windowpane of the dry box. Anthracene (3 mg, 1.68×10^{-5} mol) was then introduced into the vial under the weak red light, and the heterogeneous mixture was shaken for 10 min with the help of a small shaker placed inside the dry chamber. Since thermal degradation of the arene proceeded slowly even at room temperature and in the dark, the period of shaking was limited to 10 min, during which the degree of thermal degradation of arene was negligible. The solvent was then removed from the vial by applying vacuum in the dry box. The colored anatase particles were then transferred into a flat fused-silica cell (thickness = 2 mm, diameter = 19 mm) equipped with an inner joint. The tightly capped cell was removed from the dry box, and the diffuse reflectance spectrum of the colored anatase was quickly measured on a Shimadzu 3101-PC spectrophotometer equipped with an integrating sphere. Adsorption of other arene donors onto the anatase particles and the spectral measurements of the CT colors were carried out similarly. The procedure was repeated using inert $BaSO_4$ powder (0.7 g) as the solid support to obtain the local bands of the arene donors.

Calculation of IP(ArH) and IP[$(ArH)_2$] values. Theoretical studies have verified that arenes readily associate as dimers.[25] For instance, the exhaustive relaxed potential energy surface (PES) scans, combined with full geometry optimizations carried out at the MP2/6-31G and MP2/6-31+G levels, predicted that anthracene forms crossed (C), parallel-displaced (PD), and two T-shaped (T edge and T point) structures.[26] However, the force-field calculations predicted

only the C dimer of D_{2d} symmetry.[27] The dimer PES obtained by interacting multipolar multicenter distributions on the monomers and the valence-bond-based structures gave three structurally different dimers (PD, T edge, and T point) for the neutral and four dimers (sandwich-staggered (SS), sandwich-eclipsed (SE), PD long axis, and PD short axis) for the cationic dimers.[21]

The semiempirical AM1 method[26] was used to describe the ionization energies of the organic monomers and dimers for **1**–**5**. Both vertical and adiabatic IP(ArH) and IP[$(ArH)_2$] values were obtained by subtracting the potential energies of the most stable monomer and dimer from the corresponding cationic forms of monomer and dimer in the same geometry and from the most stable forms of the cationic monomer and dimer, respectively. No constraints were applied in the AM1 geometry optimizations.

Received: September 13, 2004
Published online: December 28, 2004

Keywords: arenes · charge transfer · physisorption · surface chemistry · titanium dioxide

[1] A. Hagfeldt, M. Grätzel, *Acc. Chem. Res.* **2000**, *33*, 269.
[2] A. Fujishima, K. Honda, *Nature* **1972**, *238*, 37.
[3] O. Legrini, E. Oliveros, A. M. Braun, *Chem. Rev.* **1993**, *93*, 671.
[4] M. A. Fox, M. T. Dulay, *Chem. Rev.* **1993**, *93*, 341.
[5] A. Fujishima, T. N. Rao, D. A. Tryk, *J. Photochem. Photobiol. C* **2000**, *1*, 1.
[6] N.-L. Wu, S.-Y. Wang, I. A. Rusakova, *Science* **1999**, *285*, 1375.
[7] M. Wagemaker, A. P. M. Kentgens, F. M. Mulder, *Nature* **2002**, *418*, 397.
[8] a) Y. Wang, K. Hang, N. A. Anderson, T. Lian, *J. Phys. Chem. B* **2003**, *107*, 9434; b) P. C. Redfern, P. Zapol, L. A. Curtiss, T. Rajh, M. C. Thurnauer, *J. Phys. Chem. B* **2003**, *107*, 11419; c) T. Rajh, L. X. Chen, K. Lukas, T. Liu, M. C. Thurnauer, D. M. Tiede, *J. Phys. Chem. B* **2002**, *106*, 10543; d) P. Persson, R. Bergström, S. Lunell, *J. Phys. Chem. B* **2000**, *104*, 10348.
[9] a) A. P. Xagas, M. C. Bernard, A. Hugot-Le Goff, N. Spyrellis, Z. Loizos, P. Falaras, *J. Photochem. Photobiol. A* **2000**, *132*, 115; b) T. Rajh, J. M. Nedeljkovic, L. X. Chen, O. Poluektov, M. C. Thurnauer, *J. Phys. Chem. B* **1999**, *103*, 3515.
[10] N. M. Dimitrijevic, Z. V. Saponjic, D. M. Bartels, M. C. Thurnauer, D. M. Tiede, T. Rajh, *J. Phys. Chem. B* **2003**, *107*, 7368.
[11] a) T. Tachikawa, S. Tojo, M. Fujitsuka, T. Majima, *Langmuir* **2004**, *20*, 4327; b) T. Tachikawa, S. Tojo, M. Fujitsuka, T. Majima, *J. Phys. Chem. B* **2004**, *108*, 5859.
[12] T. Rajh, M. C. Thurnauer, P. Thiyagarajan, D. M. Tiede, *J. Phys. Chem. B* **1999**, *103*, 2172.
[13] a) E. Vrachnou, M. Grätzel, A. J. McEvoy, *J. Electroanal. Chem. Interfacial Electrochem.* **1989**, *258*, 193; b) H. Lu, J. N. Prieskorn, J. T. Hupp, *J. Am. Chem. Soc.* **1993**, *115*, 4927; c) M. Khoudiakov, A. R. Parise, B. S. Brunschwig, *J. Am. Chem. Soc.* **2003**, *125*, 4637; d) M. Yang, D. W. Thompson, G. J. Meyer, *Inorg. Chem.* **2002**, *41*, 1254; e) Y.-X. Weng, Y.-Q. Wang, J. B. Asbury, H. N. Ghosh, T. Lian, *J. Phys. Chem. B* **2000**, *104*, 93.
[14] T. Tachikawa, S. Tojo, M. Fujitsuka, T. Majima, *Langmuir* **2004**, *20*, 2753.
[15] P. V. Kamat, *Langmuir* **1985**, *1*, 608.
[16] a) K. B. Yoon in *Handbook of Zeolite Science and Technology* (Eds.: S. M. Auerbach, K. A. Carrado, P. K. Dutta), Marcel Dekker, **2003**, 591–720; b) K. B. Yoon, *Chem. Rev.* **1993**, *93*, 321.
[17] R. S. Mulliken, *J. Am. Chem. Soc.* **1952**, *74*, 811.
[18] The lowest energy forms were assumed.
[19] a) R. Dabestani, K. J. Ellis, M. E. Sigman, *J. Photochem. Photobiol. A* **1995**, *86*, 231; b) W. E. Ford, P. V. Kamat, *J. Phys. Chem.* **1989**, *93*, 6423.
[20] A. Hagfeldt, M. Grätzel, *Chem. Rev.* **1995**, *95*, 49.
[21] B. Bouvier, V. Brenner, P. Millié, J. M. Soudan, *J. Phys. Chem. A* **2002**, *106*, 10326.
[22] J. W. Hager, S. C. Wallace, *Anal. Chem.* **1988**, *60*, 5.
[23] M. Shahbaz, I. Akiyama, P. R. LeBreton, *Biochem. Biophys. Res. Commun.* **1981**, *103*, 25.
[24] S. M. Hubig, R. Rathore, J. K. Kochi, *J. Am. Chem. Soc.* **1999**, *121*, 617.
[25] a) T. Chakraborty, E. C. Lim, *J. Phys. Chem.* **1993**, *97*, 11151; b) T. Matsuko, K. Kosugi, K. Hino, M. Nishiguchi, K. Ohashi, N. Nishi, H. Sekiya, *J. Phys. Chem. A* **1998**, *102*, 7598.
[26] C. Gonzalez, E. C. Lim, *J. Phys. Chem. A* **2000**, *104*, 2953.
[27] R. P. White, J. A. Niesse, H. R. Mayne, *J. Chem. Phys.* **1998**, *108*, 2208.

